

# EXPERIMENTAL STUDY OF SINK FLOW TURBULENT BOUNDARY LAYERS

M. B. Jones, A. E. Perry, I. Marusic and S. H. M. Hafez

Department of Mechanical and Manufacturing Engineering  
University of Melbourne, Parkville, Victoria, AUSTRALIA

## ABSTRACT

An experimental investigation of turbulent boundary layers developing in a sink flow pressure gradient was undertaken. Three flow cases were studied, corresponding to different acceleration strengths. Mean-flow measurements were taken for all three cases, while Reynolds stresses and spectra measurements were made for two of the flow cases. All the layers were found to attain a state very close to precise equilibrium. Particular interest was given to the evolution of the boundary layers, in order to test and further develop the closure hypothesis of Perry *et al.* (1994).

## INTRODUCTION

A sink flow turbulent boundary layer is one whose pressure gradient follows that of a two dimensional potential sink. A sink flow is shown in figure 1, where  $U_0$  is the reference freestream velocity at some conveniently selected origin (ie. the beginning of the boundary layer) and at  $x = L$  there exists a potential sink of strength  $Q$ . The strength of the sink can be characterised by the acceleration parameter  $K$  which is defined as

$$K = \frac{\nu}{U_1^2} \frac{dU_1}{dx} \quad (1)$$

where  $\nu$  is the kinematic viscosity and  $U_1$  is the freestream velocity. For a sink flow  $K$  remains constant and is given by

$$K = \frac{\nu}{U_0 L}. \quad (2)$$

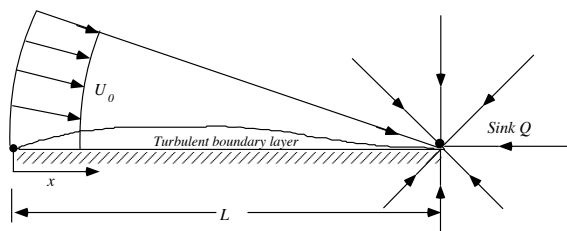


Figure 1: Sink flow.

Sink flow boundary layers are of fundamental importance, as they represent the only smooth wall boundary layer that may evolve to a state of precise equilibrium. A precise equilibrium layer is one where the mean defect velocity profiles and Reynolds stress profiles are invariant with the streamwise direction, when they are scaled with the correct velocity and length scales. This represents the most strict definition as given by Townsend (1956) and Rotta (1962).

Previous investigations of sink flows have been confined to low Reynolds number flows (eg Jones & Lauder 1972 and Spalart 1986) or focussed on the relaminarization phenomenon (eg Narayanan & Ramjee 1969 and Simpson & Wallace 1975). This study provides data at higher Reynolds numbers than past studies and also shows the full evolution of the layer to a precise equilibrium state.

## EXPERIMENTAL METHOD

Experiments were performed in an open return blower wind tunnel which has a working section length of 4.2 m. A 1.3 mm trip wire was placed the beginning of the working section and the boundary layer then developed along the smooth acrylic floor of the working section.

The pressure coefficient distribution for all experiments was controlled by a straight rigid ceiling hinged at the beginning of the working section. The pressure gradient was held fixed for all flows ( $L = 5.6\text{m}$ ) and the freestream velocity at the trip wire varied in order to achieve different acceleration strengths. Three levels of acceleration were studied:  $K = 5.4 \times 10^{-7}$ ;  $3.6 \times 10^{-7}$ ; and  $2.7 \times 10^{-7}$  which correspond to nominal velocities at the trip wire of:  $U_0 = 5.0$ ;  $7.5$ ; and  $10.0$  m/s respectively.

Mean profiles were measured using a Pitot-static probe, in conjunction with a MKS Baratron 170M-6C manometer. For each flow case 20 profiles were measured between the streamwise locations  $x = 400$  to  $x = 3620$  mm. The pitot tube readings were corrected for the effect of shear using the MacMillan (1956) correction. That is  $\delta_1/D = 0.15$ , where  $\delta_1$  is the effective location of the pitot tube above its centre line and  $D$  is the external diameter of the

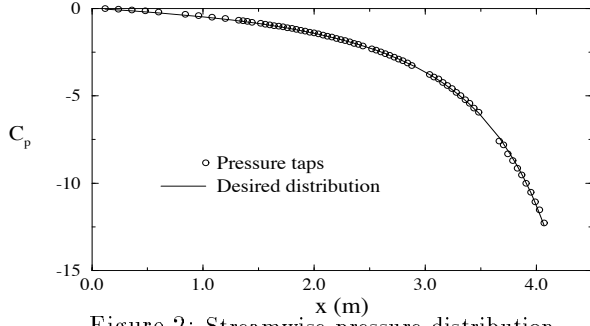


Figure 2: Streamwise pressure distribution

pitot.

The wall shear velocity  $U_\tau$  was determined by both the Clauser chart and Preston tube methods. However the Clauser chart values agreed better with momentum balances and were therefore used in favour of the Preston tube values.

Reynolds stresses were measured using constant temperature hot-wire anemometers, for the flows  $K = 5.4 \times 10^{-7}$  and  $K = 2.7 \times 10^{-7}$ . Both normal wire and cross wire probes were used, which were dynamically calibrated in a purpose built calibration tunnel prior to each traverse. The calibration was checked by shaking the probe at a known frequency. The errors in  $u_1^2$ ,  $u_2^2$  and  $u_3^2$  were within 2.0% and the errors in mean velocity were within 0.5%. Here  $u_1$ ,  $u_2$  and  $u_3$  are the fluctuating velocity components in the streamwise ( $x$ ), spanwise ( $y$ ) and wall-normal ( $z$ ) directions respectively and overbars denote temporal averages.

## RESULTS

### Mean Flow

The coefficient of pressure is defined as

$$C_p = 1 - (U_1/U_0)^2 \quad (3)$$

and for a sink flow the required distribution can be shown to be given by

$$C_p = 1 - \frac{1}{(1 - x/L)^2}. \quad (4)$$

The pressure distribution as measured by wall pressure taps is shown in figure 2 and it fits well the required distribution of (4), with  $L = 5.6\text{m}$ .

Representative mean velocity profiles for flow cases  $K = 5.4 \times 10^{-7}$  and  $K = 2.7 \times 10^{-7}$  are shown in figure 3. The mean profiles begin to exhibit similarity at approximately  $x/L = 0.6$ , for all levels of acceleration. The profiles fit well a Coles (1956) law of the wall law of the wake formulation given by

$$\frac{U}{U_\tau} = \underbrace{\frac{1}{\kappa} \ln \left[ \frac{zU_\tau}{\nu} \right]}_{\text{Law of the wall}} + A - \underbrace{\frac{1}{3\kappa} \eta^3 + \frac{\Pi}{\kappa} 2\eta^2(3 - 2\eta)}_{\text{Law of the wake}}. \quad (5)$$

In the above  $\kappa$  is the Karman constant,  $A$  is the universal smooth wall constant and  $\eta = z/\delta_c$ , where  $\delta_c$  is

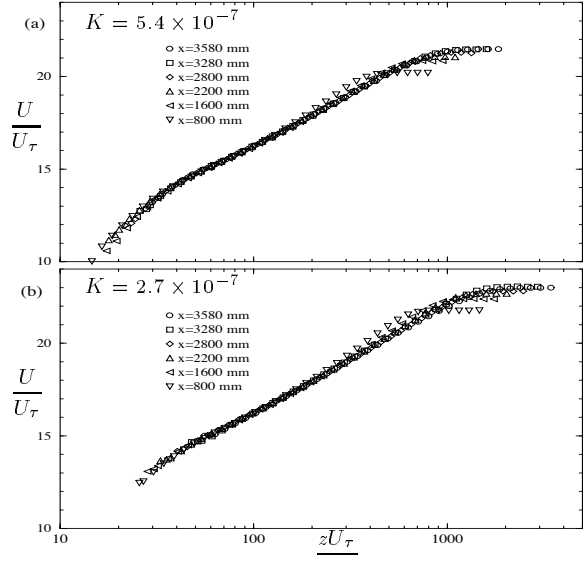


Figure 3: Law of the wall plots for; (a)  $K = 5.4 \times 10^{-7}$  and (b)  $K = 2.7 \times 10^{-7}$

the boundary layer thickness. The term  $-\eta^3/(3\kappa)$  included in (5) is required to give the correct behaviour at the edge of the layer. It is found that  $\kappa = 0.41$  and  $A = 5.0$  gives the best fit of (5) to the data. All profiles are characterised by low values of the Coles wake factor  $\Pi$ . Coles (1957) suggests that a sink flow will evolve to a ‘pure wall’ flow, that is  $\Pi = 0$ . However pure wall flow is only achieved for the highest value of  $K$ , for the other layers  $\Pi$  is small but still finite at the last station.

Figure 4 shows how the mean flow parameters:  $S$ ;  $\delta_c$ ;  $\beta$ ; and  $\Pi$  evolve, where  $S = U_1/U_\tau$  and  $\beta = (\delta^*/\tau_0)(dp/dx)$  is the Clauser (1956) pressure gradient parameter. Qualitatively the evolution of the mean flow parameters is consistent with the predicted evolution given by Perry *et al.* (1994). Rotta (1962) shows that for a precise equilibrium layer the following conditions must be satisfied

$$S = \text{constant}, \quad \frac{d\delta_c}{dx} = \text{constant}, \quad \beta = \text{constant}. \quad (6)$$

All layers appear to approach the above conditions for stations beyond approximately  $x/L = 0.6$ .

The momentum integral equation provides an method for determining the skin friction and it is given by

$$\frac{d\theta}{dx} + \frac{(H + 2)\theta}{U_1} \frac{dU_1}{dx} = C_f'/2. \quad (7)$$

In general the use of (7) is quite inaccurate since it involves differentiation of experimentally measured quantities. However for a sink flow in equilibrium  $R_\theta = \text{constant}$  in which case (7) becomes

$$R_\theta(H + 1)K = C_f'/2. \quad (8)$$

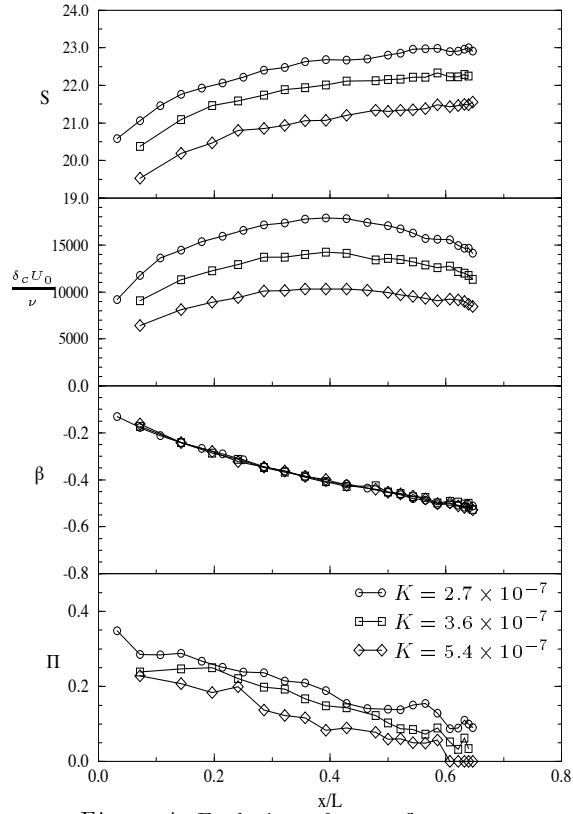


Figure 4: Evolution of mean flow parameters.

Equation (8) was used to determine the skin friction for the last measuring station. The Clauser chart values of  $U_\tau$  show good agreement with momentum values ( $\pm 1.5\%$ ) while the Preston tube values tend to be lower than the momentum values, this is opposite to the finding of Patel (1965) who claims the Preston tube will read high in favourable pressure gradients.

$K$ ( $\times 10^7$ )	Momentum $U_\tau$ (ms $^{-1}$ )	Clauser chart $U_\tau$ (ms $^{-1}$ )	% $\epsilon$	Preston tube $U_\tau$ (ms $^{-1}$ )	% $\epsilon$
2.7	1.323	1.342	+1.5	1.319	-0.3
3.6	1.035	1.026	-0.8	1.007	-2.7
5.4	0.737	0.725	-1.5	0.698	-5.2

Table 1: Wall shear velocity  $U_\tau$  calculated from momentum (8) compared with Clauser chart and Preston tube.

Equation (8) can also be used to predict the equilibrium solution. By use of (5) expressions for  $R_\theta$  and  $H$  can be generated in terms of mean flow parameter  $S$  and  $\Pi$  alone which when substituted into (8) gives

$$S^2 E \exp[\kappa S] c_1 K (-2Sc_1 + c_2) + Sc_1 = 0 \quad (9)$$

where  $c_1$ ,  $c_2$  and  $E$  are all known functions of  $\Pi$ . Using the hypothesis of Coles (1957) that  $\Pi \rightarrow 0$  for an equilibrium sink flow, the asymptotic solution for  $S$  as a function of  $K$  was determined from (9) and the result is shown in figure 5. Using (5) the other asymptotic mean flow parameters can also be found.

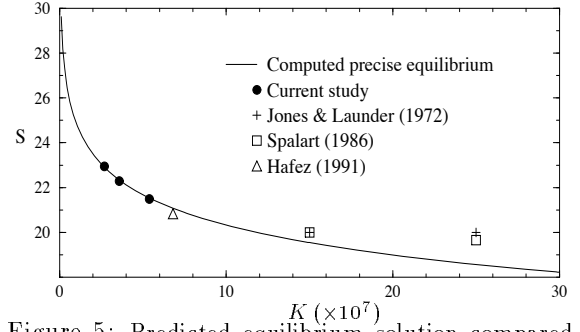


Figure 5: Predicted equilibrium solution compared to data.

In figure 5 the experimental value<sup>1</sup> of  $S$  is also shown and it shows excellent agreement with the prediction.

### Reynolds Stresses

Profiles of  $\overline{u_1^2}/U_\tau^2$  versus  $z/\delta_c$  as measured by a normal hotwire are plotted in semi-logarithmic coordinates in figure 6. For both values of  $K$  as the layer evolves the profiles of  $\overline{u_1^2}/U_\tau^2$  reduce. Similarity in  $\overline{u_1^2}/U_\tau^2$  is achieved between the last two stations ( $x = 3280, 3580$  mm) for a given  $K$  value. From cross-wire measurements it was also found that profiles of  $\overline{u_2^2}/U_\tau^2$  and  $\overline{u_3^2}/U_\tau^2$  also assumed similarity between the last two stations.

The Reynolds shear stress profiles are shown in figure 7. The development of the profiles follows the same trends for both values of  $K$ , with the profiles becoming less full as the layer evolves. The profiles of stations  $x = 3280$  and  $x = 3580$  mm appear very close to being similar.

Using the mean momentum equation and the mean continuity equation with a mean velocity profile given by the law of the wall law of the wake, Perry *et al.* have derived an expression for the total shear stress, which is given by

$$\frac{\tau}{\tau_0} = f_1[\eta, \Pi, S] + g_1[\eta, \Pi, S]\zeta + g_2[\eta, \Pi, S]\beta. \quad (10)$$

Where  $\zeta$  represents a wake strength gradient parameter given by  $\zeta = S\delta_c(d\Pi/dx)$ . Predicted Reynolds shear stress profiles were calculated by subtracting the viscous contribution from (10), which gives

$$\frac{-\overline{u_1 u_3}}{U_\tau^2} = \frac{\tau}{\tau_0} - \frac{d(U/U_\tau)}{d(zU_\tau/\nu)}. \quad (11)$$

In (11) the Reichardt (1951) profile was used to describe the mean profile in the buffer region. A typical comparison between the predicted Reynolds shear stress and data is shown figure 7 and it can be seen agreement is quite good. The other profiles give similar agreement with predicted profiles. In particular

<sup>1</sup>The average values beyond station  $x/L=0.6$  have been used.

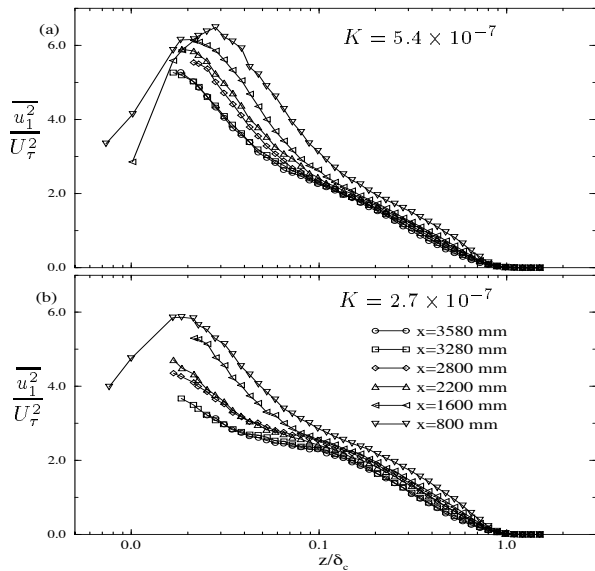


Figure 6: Streamwise turbulence intensities; (a)  $K = 5.4 \times 10^{-7}$  and (b)  $K = 2.7 \times 10^{-7}$

the measured stress is generally lower than the prediction close to the wall but is higher in the outer part of the layer.

## DISCUSSIONS AND CONCLUSIONS

The mean velocity defect profiles and Reynolds stress profiles when nondimensionalized with  $U_\tau$  show self-similarity beyond streamwise station  $x/L = 0.6$ , when plotted as a function of  $z/\delta_c$ . Therefore the layers evolve to the precise equilibrium state at  $x/L = 0.6$ , for the levels of  $K$  studied. Further the experimental mean parameters at equilibrium agree well with the solution predicted using the integral-momentum equation in conjunction with the law of the wall law of the wake.

The evolution of the mean flow parameters agrees qualitatively with the evolution predicted by Perry *et al.* (1994) and it has recently been shown by Marusic *et al.* (1998) that an extension of the method of Perry *et al.* is capable of giving good quantitative predictions of the evolution.

## REFERENCES

- Badri, M. A. Narayanan and Ramjee, V., "On the criteria for reverse transition in a two-dimensional boundary layer flow", *J. Fluid Mech.*, **35** 225-241, 1969
- Clauser, F. H., "The Turbulent Boundary Layer", *Adv. Appl. Mech.*, **4**, 1-51, 1956
- Coles, D., "The law of the wake in the turbulent boundary layers", *J. Fluid Mech.*, **1**, 191-226, 1956
- Coles, D., "Remarks on the equilibrium turbulent boundary layer", *J. Aero. Sci.*, **24**, 495-506, 1957
- Hafez, S. H. M., "The structure of accelerated turbulent boundary layers", *Ph.D. thesis, University of Melbourne, Australia*, 1991

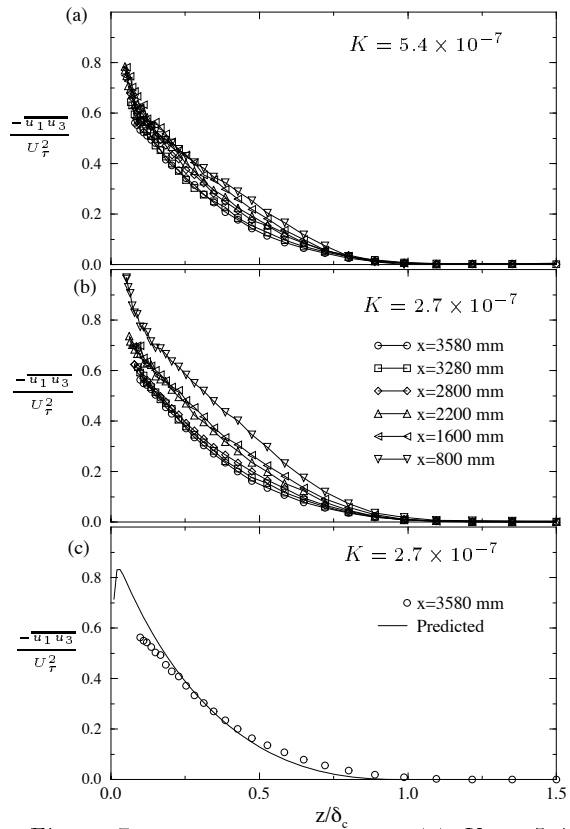


Figure 7: Reynolds shear stress; (a)  $K = 5.4 \times 10^{-7}$ , (b)  $K = 2.7 \times 10^{-7}$  and (c) an example comparison with predicted profile.

Jones, W. P. and Launder, B. E., "Some properties of sink flow turbulent boundary layers", *J. Fluid Mech.*, **56** 337-351, 1972

Marusic I., Perry A. E. & Jones, M. B., "Evolution calculations for turbulent boundary layers approaching equilibrium sink flow", *Proc. 13th Australasian Fluid Mech. Conf., Melbourne, Australia*

Patel, V., "Calibration of the Preston tube and limitations on its use in pressure gradients.", *J. Fluid Mech.*, **23** 185-205, 1965

Perry A. E., Marusic I. & Li J. D., "Wall turbulence closure based on classical similarity laws and the attached eddy hypothesis.", *Phys. Fluids*, **6** (2) 1024-1035, 1994

Reichardt, H., "Volständige darstellung der turbulenten geschwindigkeitsverteilung in glatten Leitungen", *Z. angew. Math. Mech.*, **31**, 208-219, 1951

Rotta, J. C. "Turbulent boundary layers in incompressible flow", *Prog. Aero. Sci.*, **2** 1-219, 1962

Townsend A. A. "The structure of turbulent shear flow" 1st edn. *Cambridge University Press.*, 1956

Simpson, R. L. and Wallace, D. B., "Laminar-iscent Turbulent Boundary Layers", *Project SQUID, SMU-1-PU*, 1975

Spalart, P. R., "Numerical study of sink-flow boundary layers", *J. Fluid Mech.*, **172** 307-320, 1986